Environ Earth Sci (2016) 75:554
DOI 10.1007/s12665-016-5264-7

THEMATIC ISSUE

Weathering assessment in the *Achala* Batholith of the *Sierra de Comechingones*, Córdoba, Central Argentina. II: major hydrochemical characteristics and carbon dynamics

J. O. Martínez[1] · V. A. Campodonico[1] · S. M. Fórmica[1] · P. J. Depetris[1]

Received: 29 May 2015 / Accepted: 5 November 2015

Abstract *La Trucha* is a granitic, second-order catchment (~1.9 km^2, average slope 5 %) placed at ~1400-m elevation in the *Sierra de Comechingones* (Argentina, 31°54′ S, 64°45′W; 31°53′, 64°44′W). The main geochemical characteristics were studied during a hydrological year (March 2005–February 2006), attending mainly seasonal and spatial variability and weathering-induced carbon consumption. Subjected to a *weathering-limited* denudation regime, the catchment is representative of hundreds of the second-order streams that dissect the *Achala* Batholith. Water chemistry is typical of streams draining F^- rich granites. High discharges (austral summer) determine the dilution of Na^+, Ca^{2+}, Mg^{2+}, HCO_3^-, SO_4^{2-}, and F^-. Conversely, high summer rainfall increases Cl^- concentrations. The rainfall-induced mobilization of K^+ is likely masked by its affinity for adsorption onto fine-grained particles and that of SiO_2 by its biological consumption. *La Trucha*'s upper catchment shows that steep slopes and a shallow regolith layer result in a more diluted water flow, chemically closer to rainfall. Subsurface flow increases the downriver positive rate of *La Trucha*'s electrical conductivity twice as much in winter (6.7 µS cm^{-1} per 1000 m) than during wet summer (3.9 µS cm^{-1} per 1000 m). PHREEQC allowed the calculation of free CO_2 and the likelihood of its evasion in different seasons and areas of the catchment. A mean carbon efflux of ~180 mg C m^{-2} $year^{-1}$ has been estimated for *La Trucha* catchment. The first- and second-order streams, which occupy ~62.5 km^2 of the *Achala* Batholith's surface area, are significant sources in the *Sierra de Comechingones'* carbon cycle.

Keywords Mountainous catchment · Carbon drawdown · Second-order stream · Stream geochemistry

Introduction

Continental wear away is a process that largely depends on the weathering of crustal rocks and the associated denudation regime (e.g., Depetris et al. 2014 and references therein). Weathering involves, in a synergistic way, physical, biological, and chemical aspects. Denudation, on the other hand, is a continuum of processes that spans from the *weathering-limited* regime, on one extreme, to the *transport-limited* regime on the other (Carson and Kirkby 1972). In the case of *weathering-limited* environments, the weathered material is removed more rapid than it is generated, thus little or no soil develops, and the sediments derived from these source areas are relatively unaltered. On the contrary, in basins with *transport-limited* regimes, the weathering rate exceeds the ability of transport processes to remove the material, allowing the formation of thick soils. All these processes play a significant role in the Earth's exogenous cycle, in general and, particularly, in the dynamics of carbon, because the sequestration of carbon dioxide from the atmosphere during rock weathering affects the global budget of this greenhouse gas (e.g., Berner et al. 1983). Therefore, geochemical investigations at widely differing sites have sought to differentiate the

This article is part of a Topical Collection in Environmental Earth Sciences on "3RAGSU", guest edited by Daniel Emilio Martinez.

✉ J. O. Martínez
jorgeomp@gmail.com

[1] Centro de Investigaciones en Ciencias de la Tierra (CICTERRA), CONICET-Universidad Nacional de Córdoba, Avenida Vélez Sarsfield 1611, X5016DGA Cordoba, Argentina

Published online: 25 March 2016

chemical signals of weathering in river systems with varied bedrocks. Geochemical variability stems from diverse bedrocks and from the effect of climate and its seasonal control.

Along such line and following a growing interest in mountain rivers (e.g., Wohl 2010), a year-long geochemical investigation was undertaken in a small ($\sim$1.9 km^2) mountainous granitic watershed in the *Achala* Batholith (*Sierra de Comechingones*), in Central Argentina. The first part of the study was devoted to the assessment of the characteristics of weathering in the watershed and the resulting granite-regolith fractionation (Campodonico et al. 2014). The main conclusions, associated with the prevailing *weathering-limited* regime, were that it has been dominated by physical processes that occurred at a slower rate than erosion, with little to no chemical alteration. Thus, present-day landscape remains a remnant of the conditions that predominated during Carboniferous Gondwana times (Carignano et al. 1999). Chemical mass balance calculations completed between unweathered granite and both, coarse- and fine-grained regoliths, indicated that in the coarser fraction, there were no statistically significant changes in any of the major, trace or rare-earth elements. Moreover, statistically significant losses of MgO, MnO, and P_2O_5 within the fine-grained regolith were attributed to incipient alteration of biotite and apatite (denoted by the statistical analysis of the granite-regolith fractionation); plagioclase hydrolysis was evident through microscopic examination (Campodonico et al. 2014).

In this second part of the study, the characteristics of chemical weathering are assessed in the small uniformly granitic watershed, probing whether there were similarities or differences in water chemistry attributable to climate or to spatial variability. The study in the pilot area includes, as well, the assessment of carbon efflux in the small, steep, mountainous watershed, as first- and second-order streams, which occupy $\sim$62.5 km^2 of the *Achala* Batholith's surface area, are significant sources in the CO_2 outgassing of inland freshwater systems.

Geology and climate

Geology

The small studied watershed ($\sim$1.9 km^2 and $\sim$140- m elevation), identified as *La Trucha* (Spanish for "the trout"), is located in the southern portion of the *Achala* Batholith, in the *Sierra de Comechingones* (Córdoba), Central Argentina (31°54′07″S, 64°45′28″W; 31°53′11″, 64°44′16″W) (Fig. 1). The highest peaks of the mountain range reach $\sim$2000-m elevation; the existence of bornhardts and high plains (locally known as *pampas de altura*) is an outstanding feature in the *Sierra de Comechingones*. The present-day high *sierra* resulted from the uplift on a reverse fault during an upper Tertiary stage of the Andean orogeny (e.g., Isacks 1988). The western side has steeper slopes, reaching mean values of $\sim$10 %, whereas gradients are lower on the eastern side, with slopes of $\sim$5 % (e.g., Lecomte et al. 2009).

Prevailing geology is mainly characterized by middle- to high-grade metamorphic rocks of Early Cambrian age. In some areas, Cambrian and Devonian granites are overlain by unconsolidated Early Cenozoic sediments (e.g., Siegesmund et al. 2010). The *Achala* intrusive body has a surface area of $\sim$2500 km^2, and it is the largest of a series of granitic bodies in the eastern *Sierras Pampeanas* of Argentina, which are discordant to structural features and to igneous and metamorphic rocks of early Paleozoic age. These Late Devonian granites have SiO_2 contents between 60 and 76 % and have been labeled aluminous A-type granites by Rapela et al. (2008). Lira and Kirschbaum (1990) described five petrofacies within the batholith. The dominant facies of the *Achala Batholith* (Facies B) was recognized in the drainage basin. It is a porphyritic monzogranite with K-feldspar megacrysts, plagioclase, biotite, and muscovite. Apatite, zircon, rutile, and opaque phases were identified as accessory minerals, whereas clay minerals, sericite, chlorite, and muscovite occur as secondary minerals. A more detailed geological, petrologic, and morphological description has been integrated by Campodonico et al. (2014).

Climate

The study area lies in Argentina's temperate zone, which exhibits an active atmospheric dynamics and is subjected to the action of polar and subpolar fronts. The regional climate is typically continental, with irregularly distributed atmospheric precipitation. Rainfall occurs mostly in (austral) summer and early autumn, mainly due to humid air coming in from the north. About 75 % of the total annual precipitation (a historical annual mean somewhat higher than 1000 mm) occurs between November and March. Winter (austral) is the dry season, with a mean monthly rainfall (and occasional snowfall) of $\sim$40 mm. Using the Kruskall–Wallis test (i.e., to reject the null hypothesis that states that all samples were drawn from populations with identical medians, with $p < 0.05$) and, then, the Wilcoxon non-parametric test (i.e., for comparing the medians of two matched samples, $p < 0.0001$), it was possible to separate the rainfall set into wet (October–March), and dry (April–September).

The study area is framed within the annual mean isotherm of 16 °C, dropping to about 10 °C at 2000-m elevation (Capitanelli 1979). The maximum mean isotherm is

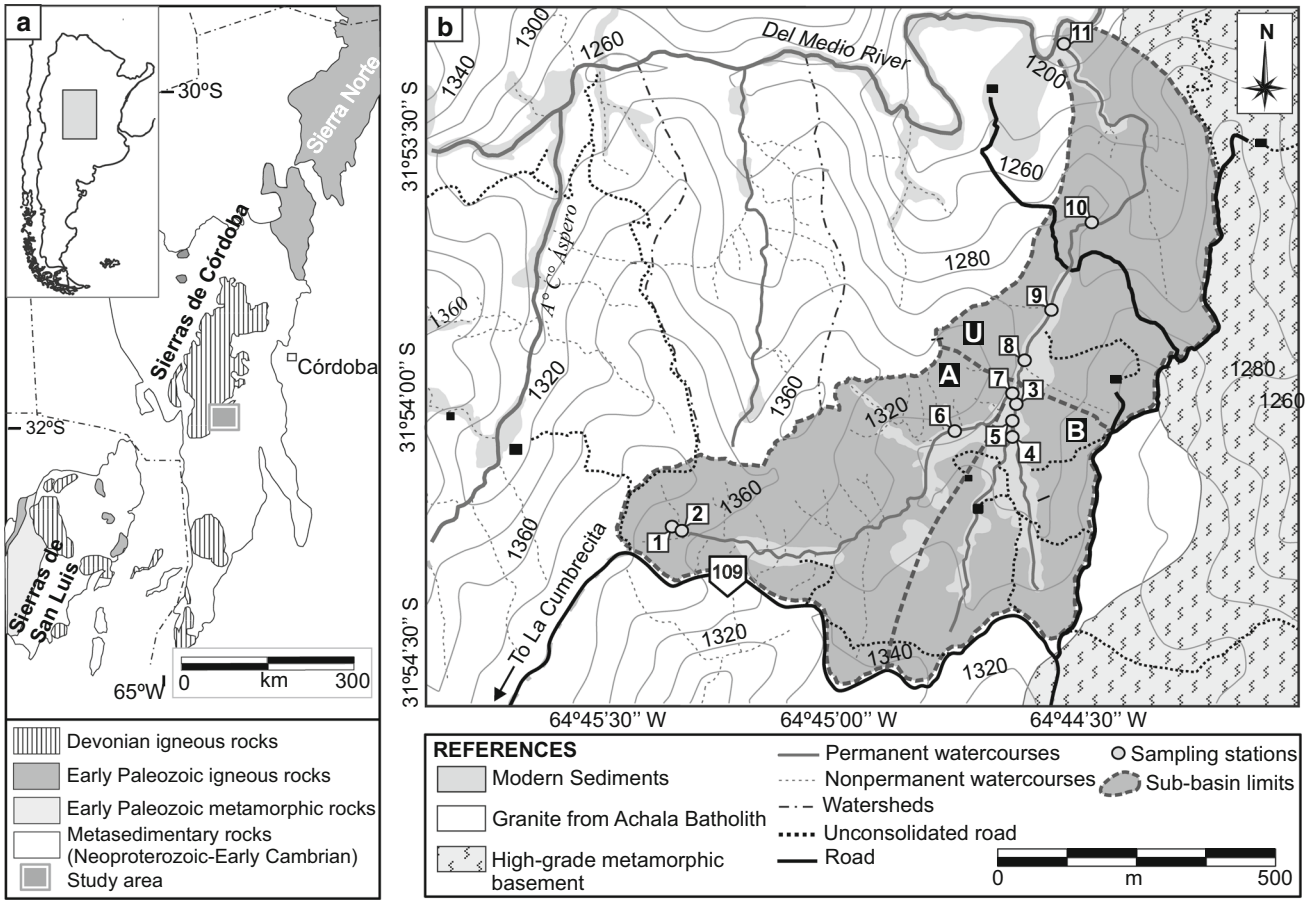

Fig. 1 **a** Location of the study area, showing the schematic regional geology (modified from Siegesmund et al. 2010). **b** Topography and geology of *La Trucha* watershed, showing the location of sampling points. Modified from Campodonico et al. (2014)

20 °C, whereas in the higher areas, it is about 14 °C. In contrast, for the lowermost areas, the minimum mean isotherm is 9 °C, whereas it is about 5 °C for the high mountainous ground. During winter, minimum temperatures can be as low as −10 °C or even lower.

The revision of recent rainfall and runoff variability in Central Argentina by means of available data series has shown that there is, in general, a significant positive trend in rainfall, which is verifiable, since the second half of the twentieth century. Moreover, spectral analysis also shows that in the studied area, south of ∼31°S (Pasquini et al. 2006), the climatic effect of El Niño-Southern Oscillation (ENSO) is a faint, but discernible and significant signal. The ENSO influence at these latitudes is not a pure signal, and there are some rainy seasons that show above-normal summer precipitation, coincidental with ENSO occurrences, and other rainy periods that are not evidently connected with ENSO events. During the 12 months (March 2005–February 2006) that took the sampling of *La Trucha*, rainfall was above the mean during the rainy season (austral summer) and was below the mean during the dry season (austral winter), even though there was not an ENSO occurrence in the equatorial Pacific Ocean (Fig. 2a). In other words, there was a noticeable change in rainfall distribution throughout the year, although the total annual precipitation (1078 mm) was not significantly different from the historical regional mean (1099 mm). The effect of rainfall on *La Trucha*'s discharges can be observed in Fig. 2b.

In spite of a considerable total annual rainfall, it turns out that relatively steep slopes, scarcely developed soils, and shallow sediment accumulations yield a scattered vegetation of grassland, wide-ranging shrubbery, and the particularly common *Parkinsoniana aculeate.*

La Trucha catchment

The small studied catchment is representative of hundreds of the first- and second-order streams—in the sense of Horton (1945) and Strahler (1952)—that constitute the upper catchments of the fluvial system that dissects the *Achala* Batholith, in Central Argentina. This

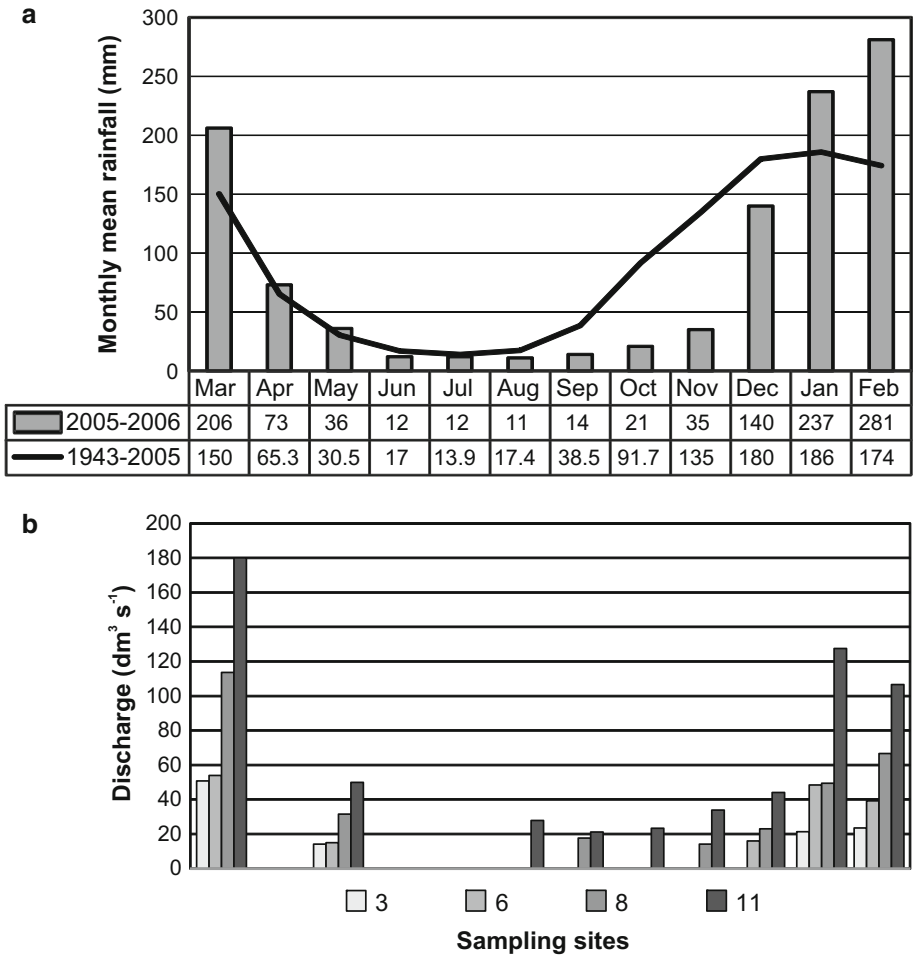

Fig. 2 *La Trucha*'s main hydrological characteristics. **a** Mean historical rainfall (*continuous line*) and rainfall recorded during the period of sampling (*bars*). **b** Stream discharge at different measuring cross sections

second-order watershed has a surface area of 1.9 km^2 and a perimeter of 7.4 km, and its drainage network is strongly controlled by the fracture pattern of the batholith. The maximum elevation in the watershed is 1374 m above the sea level, and the stream, after flowing 3500 m, reaches an outfall at *del Medio* River at an elevation of 1207 m. The mean slope of the stream bed is ~5 %, although near the mouth there are stream reaches with a channel slope of ~25 %. In the watershed, the western portion shows steeper slopes (~15 %) than the eastern side (~7 %). Therefore, a cross section of the valley shows an asymmetrical profile.

The stream has two first-order tributaries; the one draining the eastern side has been called "the A sub-basin," and the creek draining the western side "the B sub-basin" (Fig. 1). The A branch is somewhat longer than B and is also steeper. On the other hand, B flows over a thicker regolith layer (i.e., alluvium) receiving the significant water inflow from springs (V). As it will be shown, the chemical response of each tributary is noticeably different.

Field and laboratory methods

Surface water samples were collected in the studied drainage basin at 11 sampling stations (Fig. 1), to characterize the temporal and spatial variability of the dissolved load. Several samples distributed over the catchment were retrieved once a month between March 2005 and February 2006 (Table 1).

Field determinations included pH, electrical conductivity (EC), total dissolved solids (TDS), temperature, dissolved oxygen, and alkalinity measurements using standardized methods (Eaton et al. 1995). The pH was measured using a portable pH-meter with a combined electrode and integrated NTC temperature sensor for automatic temperature compensation. Electrical conductivity and TDS were measured using a portable conductivity meter, and alkalinity was determined in 100 mL samples by titration using 0.1600 N H_2SO_4 and bromcresol green-methyl red as end point indicator. Dissolved oxygen was determined by means of the modified Winkler titration method (Hach Co., Loveland, CO, USA) using a starch

Table 1 Physicochemical parameters and dissolved major ion composition (μmol L^{-1}) of samples taken at *La Trucha* catchment. Two rainfall samples are also included

Sampling	Sample	*T* (°C)	pH	EC (μS cm^{-1})	TDS (mg L^{-1})	μmol L^{-1}													DOC (mg L^{-1})	$\sum^{+}$ (μeq L^{-1})	Error (%)
						O_2	Si	Sr	Na	K	Ca	Mg	F	Cl	SO_4	HCO_3	CO_3	NO_3			
March 2005	JA1-1	17.8	6.6	34.8	16.3		356.0	0.15	180.5	5.9	42.4	7.2	72.6	17.2	12.2	200.0				285.6	−3.8
	JA1-3	21.8	7.4	55.8	28.0		409.5	0.25	252.3	17.9	99.8	21.3	82.1	28.2	16.2	389.9		6.6		512.5	1.4
	JA1-6	23.8	7.4	39.7	19.8		324.0	0.17	182.3	8.2	64.9	10.9	87.9	17.8	13.3	258.0				341.9	−5.5
	JA1-8	24.7	8.8	54.0	27.0		373.9	0.24	245.3	13.0	97.3	17.0	56.8	18.1	13.1	280.0	36.0	6.0		487.0	4.1
	JA1-10	22.3	7.5	51.0	25.5		366.7	0.22	235.8	14.1	84.8	17.2	61.1	22.6	14.9	318.0				453.9	3.6
	JA1-11	23.2	7.4	52.5	26.2		341.8	0.23	279.7	26.1	104.8	20.1	97.4	27.6	16.0	343.9				555.6	6.2
April 2005	JA2-1	12.6	7.8	37.2	18.6	224.4	373.9	0.14	187.0	4.3	47.4	7.0	52.6	19.2	12.6	261.9				300.3	−8.1
	JA2-3	14.2	7.6	55.3	27.5	258.2	341.8	0.21	231.4	14.3	87.3	18.7	90.0	30.2	16.4	370.0				457.7	−5.7
	JA2-6	14.5	7.5	45.5	22.5	231.3	391.7	0.17	211.0	9.0	72.4	11.8	59.5	14.9	13.1	296.0				388.2	0.0
	JA2-8	15.0	8.7	50.9	25.4	236.3	373.9	0.19	235.8	10.7	79.8	15.8	74.7	24.5	17.4	236.0	50.0			437.8	−2.5
	JA2-10	13.3	7.5	50.0	24.9	213.2	348.9	0.19	235.8	12.0	87.3	16.7	87.4	24.3	11.1	348.0				455.8	−1.7
	JA2-11		8.3	52.8	26.4		341.8	0.20	229.2	12.0	84.8	18.2	45.8	16.9	13.4	380.0				447.3	−1.5
May 2005	JA3-1	11.6	8.1	33.2	16.6	252.6	370.3	0.15	178.3	6.1	59.9	9.8	62.6	23.4	17.9	266.0				323.9	−8.3
	JA3-3	15.8	8.2	51.6	25.8	261.3	341.8	0.22	224.9	13.8	97.3	24.6	72.6	22.8	15.4	356.0			1.5	482.4	1.0
	JA3-6	15.3	7.9	40.0	20.0	245.1	366.7	0.17	198.3	8.7	77.3	15.2	67.9	20.3	15.8	298.0		8.4	1.1	392.1	−3.2
	JA3-8	16.1	8.5	51.1	25.5	246.3	366.7	0.20	223.6	11.3	92.3	20.3	62.6	20.9	14.4	316.0	24.0			460.1	−0.6
	JA3-10	12.8	6.8	49.2	24.6	258.8	359.6	0.20	215.3	11.0	92.3	21.4	122.6	26.2	17.4	358.0				453.7	−7.6
	JA3-11	11.5	7.2	49.9	24.9	274.5	338.2	0.21	221.4	11.3	89.8	23.6	79.0	22.3	12.7	380.0			1.2	459.5	−3.9
June 2005	JA4-1	10.7	6.4	48.0	24.0	249.5	370.3	0.17	191.0	9.0	62.4	11.3	27.9	28.8	13.3	282.7				347.2	−2.0
	JA4-3	15.5	7.0	61.0	30.5	270.1	402.3	0.25	224.9	14.6	107.3	27.8	55.3	22.6	15.1	393.9		5.6		509.6	1.3
	JA4-6	15.5	6.8	50.2	25.1	289.5	409.5	0.17	215.7	11.0	74.9	16.4	77.9	23.4	16.2	303.9				409.3	−2.2
	JA4-8	15.5	8.3	60.5	30.2	275.1	423.7	0.23	245.3	13.3	104.8	24.8	100.0	25.1	16.8	386.0				517.7	−1.3
	JA4-10	12.5	7.0	64.0	31.8	265.1	388.1	0.23	242.3	13.8	99.8	25.4	94.7	30.5	17.1	419.9				506.5	−5.4
	JA4-11	11.1	6.9	63.0	31.5	270.7	373.9	0.24	246.2	13.6	104.8	27.9	60.5	23.7	12.8	381.9				525.2	4.4
	JA4-12	16.6	6.9	311.0	156.9	131.9	445.0	1.97	1452.8	25.8	499.0	120.9	184.8	459.2	131.2	1443.7		112.9		2718.5	7.4
July 2005	JA5-1	6.3	7.6	37.5	18.7	275.1	352.5	0.16	202.3	10.5	52.4	8.7	29.5	19.7	14.6	275.5				335.0	−2.1
	JA5-3	8.5	6.8	64.4	32.1	314.5	402.3	0.27	239.7	15.3	124.8	31.0	76.3	24.3	15.5	426.0		10.3		566.5	1.0
	JA5-6	9.8	6.5	45.4	22.6	268.2	398.8	0.19	225.3	12.0	77.3	18.0	41.1	18.9	14.8	301.9				428.1	9.7
	JA5-10	8.3	7.0	57.9	28.9	273.8	377.4	0.23	242.7	12.8	112.3	27.5	89.0	24.8	16.2	406.5				535.0	−0.2
	JA5-11	6.9	7.2	58.2	29.0	330.1	348.9	0.22	235.3	13.0	104.8	27.6	89.5	23.1	20.4	396.0				513.2	−2.2
	JA5-12	14.0	7.0	315	158.2	165.7	437.9	1.91	1435.4	25.1	499.0	118.9	144.2	363.0	112.6	1601.8		204.0		2696.2	5.4
August 2005	JA6-1	6.6	6.6	38.4	19.2	268.8	341.8	0.15	232.3	11.0	74.9	10.5	63.2	17.8	13.6	278.0				414.0	4.0
	JA6-3	13.8	8.0	62.2	31.1	310.7	405.9	0.27	257.1	15.3	122.3	29.2	91.1	21.4	16.6	399.9				575.4	3.9
	JA6-6	14.9	6.6	50.0	25.0	274.5	413.0	0.18	230.1	11.0	82.3	19.1	99.0	23.4	10.8	313.9				444.0	−0.4
	JA6-8	12.8	8.8	60.6	30.2	321.4	462.9	0.23	295.3	14.3	124.8	27.5	111.1	21.7	20.2	298.0	54.0			614.2	6.7
	JA6-10	9.1	6.9	62.0	31.0	303.2	395.2	0.26	267.5	13.6	122.3	28.6	103.2	22.0	14.9	421.9				582.8	1.8
	JA6-11	8.1	7.0	61.0	30.6	310.7	359.6	0.25	263.2	13.0	122.3	30.3	81.1	24.3	10.1	421.9				581.3	4.1
	JA6-12	15.2	6.6	315.0	157.0	168.2	427.3	1.87	1444.1	24.3	499.0	115.6	119.0	258.1	85.4	1557.8		146.8		2697.6	11.4
	JA7-1	10.3	6.4	37.3	18.6	268.8	242.1	0.16	181.4	11.0	62.4	11.4	30.5	21.7	14.2	263.9				340.0	0.0

Table 1 continued

Sampling	Sample	T (°C)	pH	EC (μS cm^{-1})	TDS (mg L^{-1})	μmol L^{-1}													DOC (mg L^{-1})	$\sum^{+}$ (μeq L^{-1})	Error (%)
						O_2	Si	Sr	Na	K	Ca	Mg	F	Cl	SO_4	HCO_3	CO_3	NO_3			
September 2005	JA7-3	17.5	8.1	60.3	30.1	292.0	388.1	0.23	251.0	13.6	112.3	27.6	115.8	24.3	17.6	406.0				544.3	−2.1
	JA7-6	16.6	6.3	46.3	23.2	262.6	402.3	0.17	221.0	10.0	87.3	17.4	60.5	22.8	11.0	310.0		11.2		440.4	2.8
	JA7-8	18.1	7.9	58.1	29.0	280.1	416.6	0.22	277.1	12.5	109.8	25.5	98.4	20.0	10.1	381.9				560.2	4.9
	JA7-10	12.5	6.8	58.1	29.0	280.7	363.2	0.23	245.3	11.5	107.3	25.9	83.7	25.7	14.2	419.9				523.2	−1.9
	JA7-11	12.1	6.6	59.0	29.5	276.3	324.0	0.24	254.9	12.0	112.3	29.1	50.0	18.1	12.3	439.9				549.6	2.7
October 2005	JA8-2	14.6	6.5	58.2	29.1	294.5	427.3	0.19	288.4	7.7	99.8	26.2	107.9	20.6	10.2	443.9				548.1	−2.9
	JA8-3	21.8	6.8	62.6	31.3	258.2	462.9	0.21	306.7	7.7	99.8	29.7	111.6	23.1	17.6	438.0			1.0	573.4	−2.0
	JA8-6	18.8	6.2	50.5	25.3	230.7	462.9	0.16	268.4	9.2	74.9	18.3	120.0	25.4	14.1	338.0			1.6	463.8	−0.4
	JA8-8	22.1	6.7	63.1	21.8	275.7	427.3	0.23	309.3	8.4	99.8	29.4	62.1	18.1	12.4	436.0				576.0	4.2
	JA8-10	18.3	6.6	61.2	30.7	244.5	391.7	0.22	312.3	9.0	99.8	28.5	69.0	18.6	15.7	439.9				577.8	2.8
	JA8-11	18.7	6.6	67.1	33.6	266.3	334.6	0.28	354.5	13.8	124.8	36.4	61.6	18.9	13.7	493.9		8.5	1.5	690.7	7.1
	JA8-12	18.4	6.7	316	159.5	128.2	534.0	2.04	1522.4	28.1	499.0	128.8	118.4	258.9	85.5	1661.7		131.3		2806	11.4
November 2005	JA9-3	23.2	6.6	57.7	28.8	234.4	359.6	0.25	245.8	10.5	107.3	26.6	89.5	21.4	15.9	438.0				524.0	−4.2
	JA9-6		7.9	43.3	21.5	209.4	292.0	0.18	172.2	7.2	77.3	14.4	84.2	17.5	14.1	308.0				362.8	−8.4
	JA9-8	25.2	7.6	59.2	29.5	192.6	331.1	0.22	247.5	11.3	104.8	21.8	76.3	19.2	14.8	391.9				512.0	0.7
	JA9-10	20.0	7.0	53.3	26.6	217.6	309.8	0.22	214.0	11.8	94.8	20.9	97.9	18.9	12.7	356.0				457.3	−3.1
	JA9-11	20.3	7.0	52.9	26.5	212.6	288.4	0.22	205.7	10.0	94.8	24.0	100.5	21.4	16.3	393.9		5.0		453.3	−8.9
December 2005	JA10-1	19.9	6.4	26.4	13.2	211.9	302.6	0.12	158.8	5.1	49.9	8.3	86.9	15.5	11.6	171.9				280.2	−2.0
	JA10-3	24.0	6.5	56.3	28.1	203.8	391.7	0.25	291.4	15.1	124.8	28.6	69.5	24.5	13.8	413.9			2.2	613.3	7.8
	JA10-5	17.2	6.1	69.1	34.3		605.3	0.26	361.0	18.7	149.7	36.5	106.3	24.8	18.3	473.9		22.1		752.1	7.5
	JA10-6	24.7	6.4	36.3	18.1	199.4	313.3	0.14	197.9	9.7	74.9	12.0	82.6	17.5	11.1	298.0			3.1	381.4	−3.9
	JA10-8	25.0	6.5	48.1	24.0	194.4	391.7	0.21	260.5	13.0	99.8	21.8	76.3	18.6	13.0	363.9				516.7	4.3
	JA10-10	19.9	6.3	33.3	16.6	206.9	259.9	0.15	172.2	15.3	74.9	16.2	100.0	18.3	9.8	256.0				369.6	−2.0
	JA10-11	19.9	6.1	32.4	16.2	212.6	217.2	0.14	158.3	15.6	74.9	16.2	35.3	17.2	9.9	201.9		5.0	3.3	356.1	13.3
January 2006	JA11-1	19.8	7.1	25.9	12.9	244.5	327.6	0.11	171.8	5.1	49.9	7.7	70.5	19.2	10.9	213.9				292.0	−4.5
	JA11-3	22.1	7.1	50.2	25.1	215.7	427.3	0.22	248.8	15.9	99.8	23.0	53.2	23.7	11.5	360.0				510.3	6.2
	JA11-5	18.9	7.4	69.8	34.8	136.9	605.3	0.26	353.2	18.4	149.7	38.3	80.0	20.0	17.0	483.9		5.0		747.7	10.5
	JA11-6	23.0	7.4	32.2	16.1	222.6	299.1	0.13	166.6	7.9	49.9	10.8	92.1	20.6	11.8	268.0				295.9	−14.4
	JA11-8	25.5	6.1	41.8	20.8	187.6	356.0	0.18	215.3	11.5	74.9	16.9	80.5	25.9	15.2	303.9				410.3	−2.5
	JA11-11	20.2	6.2	41.9	20.9	222.6	338.2	0.17	199.7	13.6	74.9	20.2	91.6	27.1	16.0	280.0				403.2	−2.0
	JA11-12	18.4	6.9	325.0	163.0	136.9	534.1	1.95	1522.4	306.9	499	121.8	134.8	381.9	111.2	1751.7		121.3		3070.8	6.3
February 2006	JA12-1	18.4	6.3	26.3	13.1		324.0	0.12	164.0	5.1	49.9	7.7	28.4	22.0	12.0	208.0				284.2	1.1
	JA12-3	21.1	6.1	48.2	24.1		356.0	0.22	211.0	21.0	99.8	22.5	108.4	32.2	10.2	306.0			2.4	476.5	2.1
	JA12-5	18.3	6.2	68.1	34.1		569.7	0.26	318.0	17.1	149.7	34.8	76.9	20.3	11.3	478.0				704.1	9.4
	JA12-8	23.0	7.3	40.5	20.2		316.9	0.18	183.6	14.6	99.8	17.0	71.1	25.1	14.0	271.9				431.8	5.3
	JA12-10	19.0	7.8	33.4	16.6		242.1	0.16	147.9	17.9	74.9	15.4	72.6	28.2	15.1	245.0		9.7		346.3	−4.3
	JA12-11	19.6	6.2	33.5	15.6		231.4	0.16	149.6	19.2	74.9	17.6	75.8	24.3	13.0	210.0			3.9	353.8	3.6
Sept-Oct 2001	LL-LR2-K[a]	nd	6.7	nd	3.1	nd		nd	21.0	10.0	8.0	7.0		17.0	11.0	8.0					10.0

Table 1 continued

Sampling	Sample	*T* (°C)	pH	EC (μS cm^{-1})	TDS (mg L^{-1})	μmol L^{-1}												DOC (mg L^{-1})	$\sum^{+}$ (μeq L^{-1})	Error (%)
						O_2	Si	Sr	Na	K	Ca	Mg	F	Cl	SO_4	HCO_3	CO_3	NO_3		
Jan-Feb 2006	LL-12J	nd	5.2	19.1	9.5	nd	<7.0	nd	17.0	7.7	<17.5	2.0	55.8	16.9	11.4	nd				

EC electrical conductivity, *TDS* total dissolved solids, *nd* not determined

[a] Rainfall sample reported in Lecomte et al. (2005)

indicator solution and titration with sodium thiosulfate (0.2000 N) to a colorless end point.

At six sampling stations, monthly surface water samples were filtered through 0.22-μm cellulose acetate membrane filters (EMD Millipore, Billerica, MA, USA) and divided into two aliquots. The filtration equipment was repeatedly rinsed with sample water prior to filtration. One aliquot (50 mL) was acidified to pH <2 with ultrapure HNO_3 (>99.999 %, redistilled, Sigma-Aldrich Corp., St. Louis, MI, USA) and stored in precleaned polyethylene bottles for the analytical determinations of major cations and trace elements. The other aliquot (500 mL), used for the determination of major anions, was stored at 4 °C in precleaned polyethylene bottles, without the acid addition.

Major anions (NO_3^-, F^-, Br^-, Cl^-, SO_4^{2-}, and PO_4^{3-}) were determined by chemically suppressed ion chromatography with conductivity detection. Major cations and trace elements were measured by ICP-MS (Perkin Elmer Sciex Elan 6000—quadrupole mass spectrometer) at Activation Laboratories Ltd. (ACTLABS, ON, Canada). For most of the analyzed stream waters, the charge imbalance between cations and anions was less than 10 %. The results for major and trace elements were validated with NIST-1640 (National Institute of Standards and Technology, USA) and SRLS-4 (National Research Council of Canada), and carried out along with sample analysis. In addition, duplicated analyses were performed every ten samples to check the reproducibility of results.

Dissolved organic carbon (DOC) was determined in an external laboratory (Aguas Cordobesas, Córdoba, Argentina) in twelve representative samples by means of a carbon analyzer.

Discharge measurements were performed during seven sampling campaigns at four sampling stations. The velocity-area method (e.g. Serrano 1997) was used to estimate the discharge at each station, measuring section area and flow velocity (by means of floaters).

The carbon efflux for *La Trucha* catchment was estimated through inverse modeling with PHREEQC, using the phreeqc.dat thermodynamic database (Parkhurst and Appelo 2013), and discharge measurements. This approach begins with a known initial solution and available mineral phases, and quantifies the processes that lead to the final solution chemistry. For this purpose, it reconstructs all possible combinations of dissolution and/or precipitation reactions that explain the chemical changes observed between the two solutions and the mineral phases. The climatic aspects, the topographic differences, and its relationship with the flow patterns were considered in the inverse models.

Results and discussion

Main hydrochemical characteristics

Table 1 shows the physicochemical parameters and the major ion composition of surface waters in *La Trucha* catchment. Two composite rainfall samples from Villa Berna (31°54′43″S 64°43′35″W) are also included in Table 1. Sample LL-12J was retrieved between January and February 2006, whereas sample LL-LR2-K reported by Lecomte et al. (2005) corresponds to September and part of October 2001.

Circumneutral to slightly alkaline conditions prevailed along the small drainage basin, with a mean pH of 7.24 ± 0.79. The average alkalinity of surface waters was 349.67 ± 70.22 μeq L^{-1}, and it is attributed mainly to the presence of HCO_3^-, because pH values rarely exceeded 8.23. The average electrical conductivity (EC) and total dissolved solids (TDS) values measured in the analyzed stream waters were of 49.95 ± 10.21 μS cm^{-1} and 24.92 ± 5.14 mg L^{-1}, respectively.

The lowest values of EC, TDS, and alkalinity were measured during the wet season when waters were significantly diluted. In general, pH was circumneutral or slightly acid during the wet season with a marked alkaline trend during the dry season. The dynamics of water pH suggests that, besides the hydrolysis of silicates, other mechanisms, such as organic matter decomposition, may affect its variability.

The ionic composition at *La Trucha* was dominated by Na^+, Ca^{2+}, HCO_3^-, and F^-, which accounted for ~89 and ~90 % of the total concentration of major cations and anions, respectively. Fluorapatite and biotite are probably the main mineral phases responsible for the relatively high dissolved concentrations of F^-. According to Piper's (1944) water classification, samples were predominantly of the Na^+–K^+ to Na^+–K^+–Ca^{2+}-type, and of the HCO_3^--type (Fig. 3). The headwaters (sub-basin A) showed slightly lower concentrations of Cl^- and SO_4^{2-}, when compared with the other sub-basin (B), probably reflecting the chemical signature of rainwater (Table 1).

The total sum of cations ($\sum^+$, Table 1) shows that *La Trucha* falls into the *dilute* ($750 < \sum^+ < 375$ μeq L^{-1}) or *very dilute* ($375 < \sum^+ < 185$ μeq L^{-1}) water-type categories in Meybeck's (2005) idealized model of river chemistry.

To identify the possible sources of dissolved elements, several molar ratios were calculated and compared with the stoichiometric ratios on dissolution and hydrolysis reactions in rock-forming minerals (Fig. 4). The Cl^-/Na^+ and SO_4^{2-}/Ca^{2+} molar ratios do not show significant

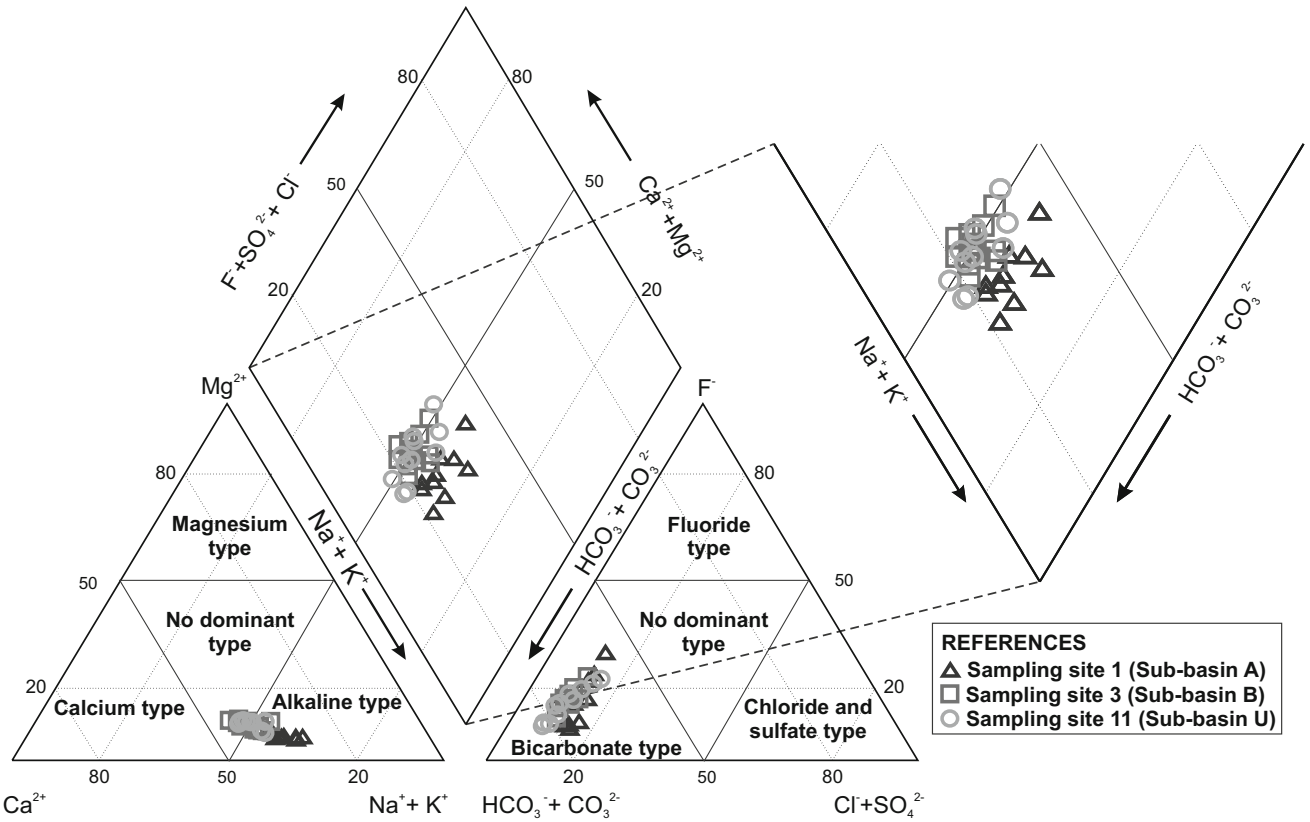

Fig. 3 Piper's diagram showing the main hydrochemical characteristics of the studied catchment

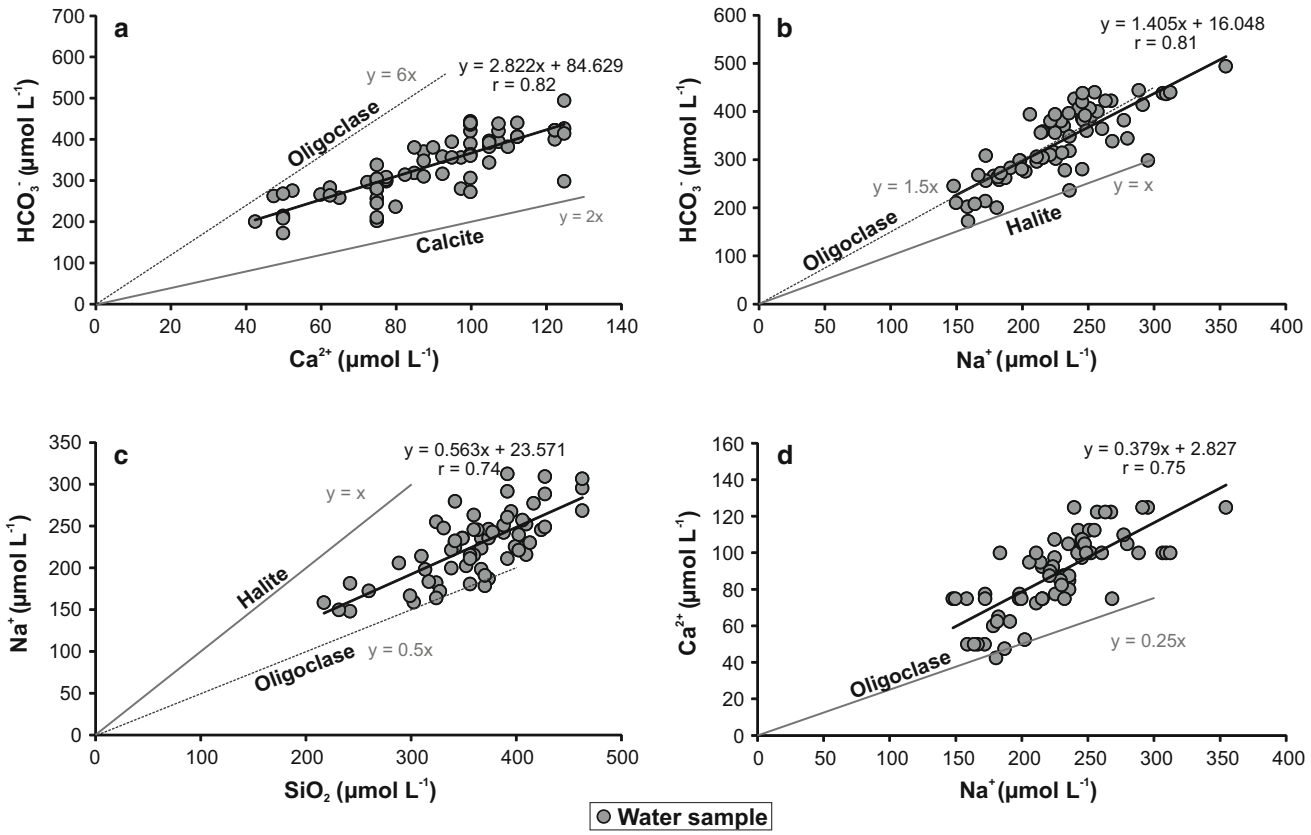

Fig. 4 Main ionic relationships at *La Trucha* catchment. **a** HCO_3^- vs. Ca^{2+}. **b** HCO_3^- vs. Na^+. **c** Na^+ vs. SiO_2. **d** Ca^{2+} vs. Na^+

correlations, suggesting that neither evaporite dissolution nor rainfall exerts a clear control over the concentration of these major ions. Therefore, the major ion composition of the dissolved load may be affected by the presence of other mineral phases in the *Achala* Batholith, such as oligoclase, mica, fluorite, fluorapatite, or calcite (Lecomte et al. 2005, 2011). The HCO_3^-/Ca^{2+} molar ratio shows a significant correlation ($r = 0.82$; $p < 0.001$), and stream waters plot between the theoretical dissolution segments for oligoclase and carbonates, indicating the presence of other mineral sources besides plagioclase (Fig. 4a). On the other hand, the HCO_3^-/Na^+ molar ratio shows a significant correlation ($r = 0.81$; $p < 0.001$), and the slope of the regression line (1.41) is similar to the slope of the theoretical dissolution of oligoclase (1.5), mainly during the rainy season, thus suggesting that the hydrolysis of this mineral is the main source of Na^+ and alkalinity (Fig. 4b). Similarly, the relationship Na^+/SiO_2 ($r = 0.74$; $p < 0.001$) is also close to the theoretical dissolution of oligoclase (slope = 0.5), with a slope of 0.56 (Fig. 4c). In addition, the water samples have a Ca^{2+}/Na^+ molar ratio of ~0.38 (Fig. 4d). This value is consistent with the ones calculated by Oliva et al. (2004) in stream waters draining granitic environments ($Ca^{2+}/Na^+ < 1$), and by Gaillardet et al. (1999) for the silicate end-member ($Ca^{2+}/Na^+ = 0.35$).

Figure 5 (modified from Oliva et al. 2004) shows the relationship between Mg^{2+}/Na^+ and Ca^{2+}/Na^+ molar ratios, which allows the determination of the relative

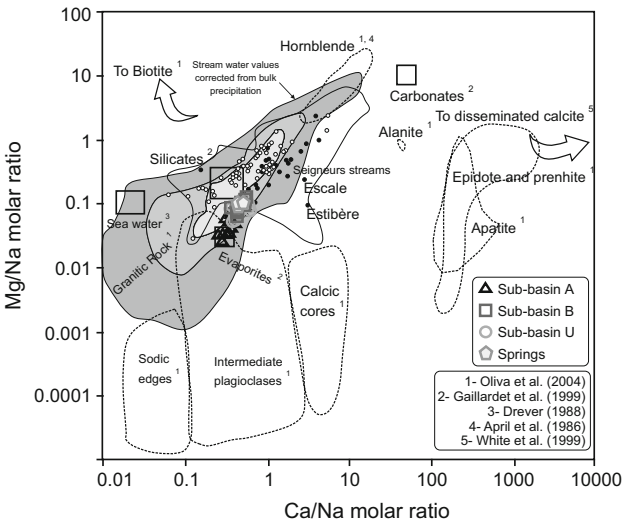

Fig. 5 Ca/Na vs. Mg/Na diagram, modified from Oliva et al. (2004). Samples from *La Trucha* are included. The *gray* domains represent granitic rocks, and *filled points* represent high elevation watersheds (above 1500 m of elevation). Other details on the diagram can be found in Oliva et al. (2004)

contribution of the different lithologies to water chemistry. Open circles correspond to small watersheds draining granitic terrains, and filled circles correspond to waters from high elevation systems (mountainous, >2000 m elevation) (Oliva et al. 2004). The granitic domain was defined by these authors using Mg^{2+}/Na^{+} and Ca^{2+}/Na^{+} ratios from more than 200 granitic rocks from all over the world. The mineralogical domains for plagioclases, epidote and prehnite, apatite and hornblende, and the directions for biotite and disseminated calcite domains are also shown in Fig. 5. As expected, the stream waters from this study plot within the granitic domain, indicating that the dissolved load is mainly supplied by granite weathering (Fig. 5). Moreover, the analyzed waters are clustered in the right part of the "small watershed set," coincident with mountainous stream waters (filled points). In contrast, Oliva et al. (2004) pointed out that in high elevation systems, where the ratio $Ca^{2+}/Na^{+} > 1$, the chemical weathering of trace minerals, such as calcite, apatite, and epidote, can have a major influence on stream water chemistry.

The seasonal variability of major chemical components

Although there are four clear-cut seasons at the *Sierra de Comechingones* from the atmospheric precipitation regime standpoint, there are two statistically significant seasons at *La Trucha*: wet or rainy, mostly during the austral summer and at the beginning of fall (from October until March) and dry, from April until September. During the wet period, precipitation reaches a mean total of 917 mm (~83 % of the total annual rainfall), and during the dry season, it amounts 183 mm (the remaining ~17 %). Stream base flows, in wintertime, oscillate between 15 and 25 L s^{-1}, and mean discharge may increase tenfold during the wet summer. Intense episodic events during summertime determine torrential floods that probably peak at ~1 m^3 s^{-1} and last for several hours.

The geochemical response of the system to water availability is clear: relatively high conductivity/TDS at base flow, between June and November (50–60 μS cm^{-1} or 25–30 mg L^{-1}); low concentrations at high flow, between December and February (~40 μS cm^{-1} or 15–20 mg L^{-1}), and intermediate values during March–May (~47 μS cm^{-1} or 24 mg L^{-1}), showing the "memory effect" of the wet period subsurface flow.

There is a group of ionic components that show a clear association with the diluting action of rainfall. Na^{+}, Ca^{2+}, and Mg^{2+}, among cations, are clearly less concentrated during summer (i.e., high discharge), and HCO_3^{-}, SO_4^{2-}, and F^{-} follow this pattern (Fig. 6). Cl^{-} does not reflect a seasonal periodicity, although its connection with rainfall is reflected by the concentration increase triggered by the precipitations of January and February. The adsorption–desorption mechanism of K^{+} is clearly stronger than the diluting effect of increased subsurface flow, and hence, this cation does not show a significant seasonal trend. In contrast, the biogeochemical control is less efficient than the diluting action of rainfall, and hence, dissolved SiO_2 shows a concentration decrease during the wet summer (Fig. 7).

Spatial variability of major chemical components

As pointed out above, the sub-basins A and B exhibit different characteristics, which have an effect on the chemical response of each tributary. The chemical signature of the tributaries is basically determined by the residence time that water (i.e., subsurface flow) has in each particular sub-basin. Figure 8 shows that A has lower mean TDS and alkalinity concentration, and it has a higher pH than B. The chemical impact of spring inflows (V) is clearly visible. *La Trucha* main stem (U) reaches intermediate mean values for the three considered parameters before reaching its outfall at *del Medio* River.

Major chemical components in streams not only show variability attributable to changes in seasonal water supply (e.g., important dilution, sometimes caused by overland flow during summer storms), but also exhibit concentration changes along their course as flow increases mostly due to subsurface flow or, much less likely, due to groundwater flow. It is a known fact that in steep, rocky mountain streams, the groundwater contribution to surface flow often is not significant (Manning 1987). In small streams, as is the case of *La Trucha*, the hydrochemical dynamics can be followed more closely than in larger rivers, which generally drain varied lithologies and climate regimes (e.g., Oliva et al. 2003).

Figure 9a shows the mean annual downstream variation of electrical conductivity. The positive trend toward the mouth—typical of small and steep mountainous catchments—indicates that the stream water is progressively concentrated at a mean rate of ~5.6 μS cm^{-1} per 1000 m. The introduction of the seasonal component in the analysis (Fig. 9b) shows that, as expected, the stream water is more diluted in summer (i.e., rainy season) than in winter (i.e., dry season). Surely determined by the contribution of subsurface flow, the electrical conductivity increases less rapidly (3.9 μS cm^{-1} per 1000 m) in summer than in winter (6.7 μS cm^{-1} per 1000 m), when the subsurface flow is more concentrated. The regression line crosses the y-axis at the headwaters (Fig. 9a), where the initial spring outcrops, with a mean electrical conductivity of 35.3 μS cm^{-1} in summer and 41.9 μS cm^{-1} in winter. These values are significantly higher than the electrical conductivity of rainfall (a mean 19.1 μS cm^{-1} was measured for the January–February 2006 rainy period;

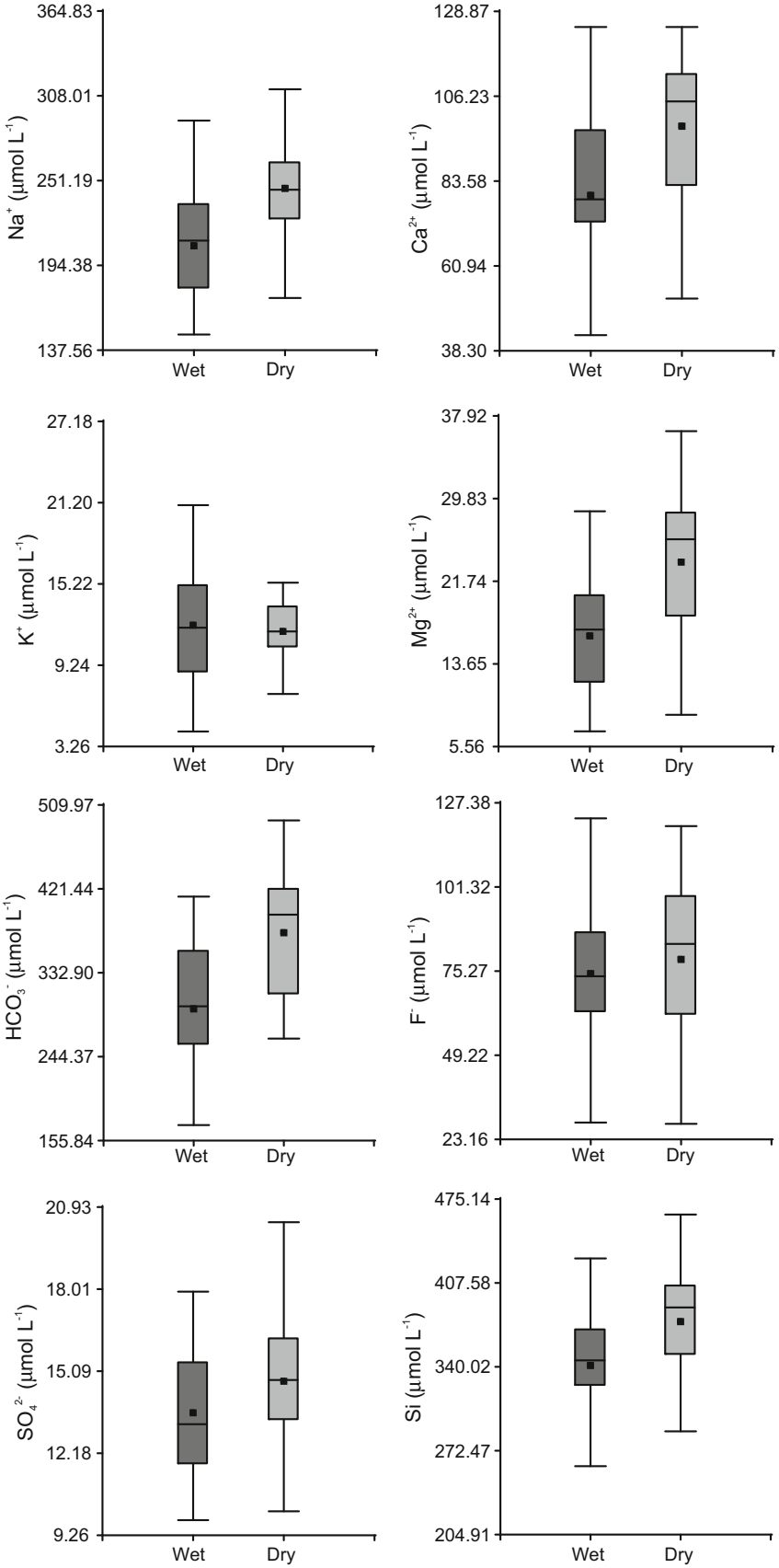

Fig. 6 *Box* and *whisker diagrams* show the distribution of major ions and silicon in waters from *La Trucha* catchment during wet and dry seasons

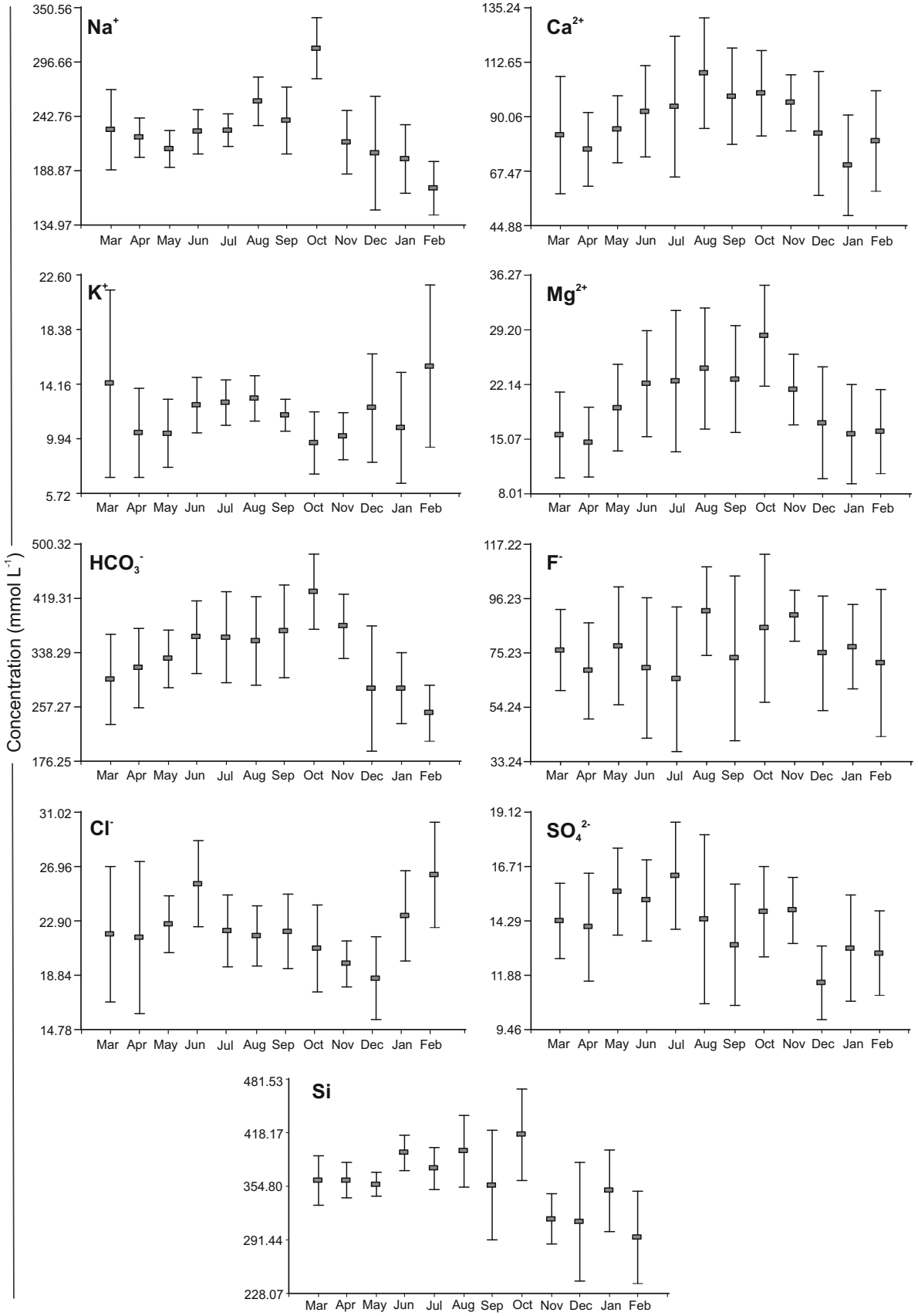
Concentration (mmol L-1)
Na+
350.56
296.66
242.76
188.87
134.97
Ca2+
135.24
112.65
90.06
67.47
44.88
K+
22.60
18.38
14.16
9.94
5.72
Mg2+
36.27
29.20
22.14
15.07
8.01
HCO3-
500.32
419.31
338.29
257.27
176.25
F-
117.22
96.23
75.23
54.24
33.24
Cl-
31.02
26.96
22.90
18.84
14.78
SO4 2-
19.12
16.71
14.29
11.88
9.46
Si
481.53
418.17
354.80
291.44
228.07
Mar Apr May Jun Jul Aug Sep Oct Nov Dec Jan Feb

◀**Fig. 7** *Box* and *whisker diagrams* show the monthly distributions of major ions and silicon in waters from *La Trucha* catchment

Table 1), thus implying that the residence time of spring water within rock cracks and in the regolith is long enough to double the solutes concentrations.

It is interesting to examine the spatial variability of mean concentration of individual ionic species and silicon (Fig. 10). Not surprisingly, Na^+, Ca^{2+}, Mg^{2+}, and HCO_3^- are more diluted during the rainy season, and the slopes of the linear trends are lower, thus implying that the solute supply of these ions through subsurface flow is more diluted during the wet season than during the dry season.

Sodium is mostly supplied by the hydrolysis of plagioclase and, also, has a significant source in rainfall. Rainwater in the region has Na^+ concentrations in the range of 15–30 μmol L^{-1} and has been recognized as a dominant cation in rain and spring waters (Lecomte et al. 2009). The absence of a statistically significant concentration trend in the downstream direction during the wet season is probably linked to the chemical signature of rainwater, which is likely transferred to the subsurface flow. Rivers and streams of this mountainous region preserve the Cl^- signature of atmospheric precipitations (Lecomte et al. 2009), and Na^+ probably follows the trend (Fig. 10).

Potassium ion is special in the sense that it only exhibits a significant trend during the rainy summer, whose slope is 2.9 times lower than, for instance, Ca^{2+}, in agreement with the slow dissolution kinetics of its likely main sources (K-feldspar and muscovite). During the dry winter, subsurface flow is lower, and the residence time of water flowing through rock fractures and in regolith pores is longer, thus increasing the likelihood that K^+ is adsorbed. Hence, in winter (i.e., dry period), concentrations remain relatively constant throughout the sampled stream reach (Fig. 10).

Chloride does not show a significant trend in coherence with its well-known conservative nature; as pointed out above, it probably carries the chemical signal of rainfall. Keeping in mind that the *Achala* Batholith is composed of an F-rich granite, it must be concluded that F^- is probably affected by point-sources (i.e., springs) with higher F^- concentrations, thus altering (i.e., diluting) the trend exhibited by other elements. Likewise, the main source of SO_4^{2-} is, probably, the oxidation of pyrite concentrated in restricted spots in regolith accumulations, and the downstream concentration trend is almost certainly controlled as in the case of F^- by point-sources. Finally, Si concentrations are usually regulated by biogeochemical mechanisms, such as consumption by fresh water algae and sponges, and therefore, its concentration trend in the studied stream reach is not statistically significant (Fig. 10). Streams and

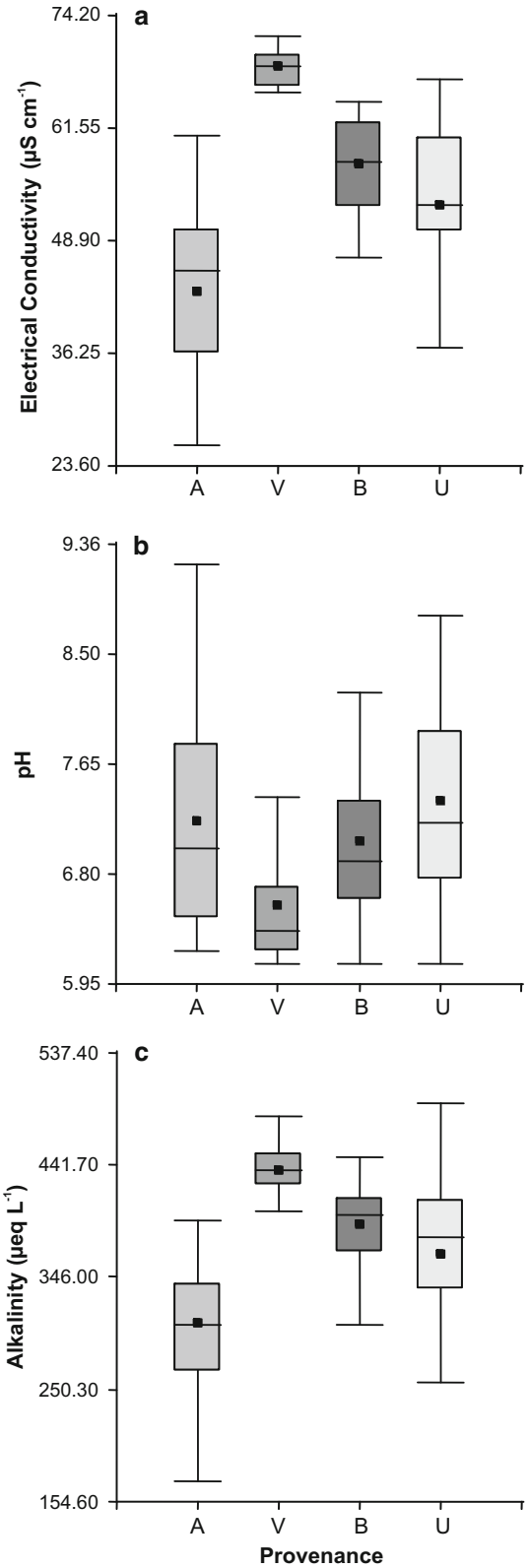

Fig. 8 *Box* and *whisker diagrams* show the distribution of **a** electrical conductivity, **b** pH, and **c** alkalinity in the sub-basins of *La Trucha* watershed. *A* sub-basin A, *V* springs, *B* sub-basin B, and *U* sub-basin U

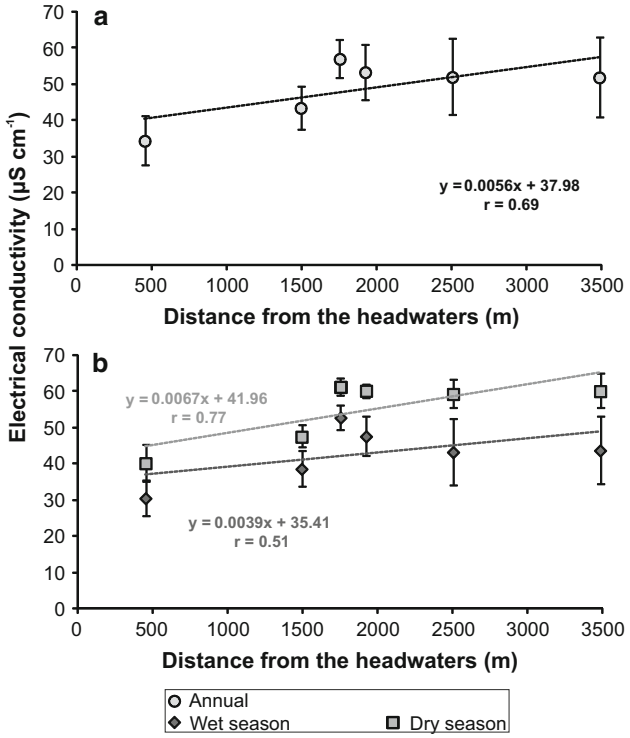

Fig. 9 Downstream variation of electrical conductivity in *La Trucha* catchment. **a** Annual, and **b** Seasonal

rivers in the *Sierra de Comechingones* are often mesotrophic in their upper reaches, with significant periphyton and algal drift, particularly Si-consuming diatoms (Gari and Corigliano 2004). The substantial biodiversity of such mountainous temperate streams has been recently underlined (Daga et al. 2014).

Carbon dynamics

Carbon is a ubiquitous and dynamic chemical element that mediates between Nature's different compartments. The carbon cycle and its permanent influence on climate through the weathering of silicate rocks (Berner et al. 1983) uphold a persistent scientific interest in the riverine dynamics of carbon. Currently, the air of the atmosphere contains about 400 ppmv CO_2. Rainwater is in equilibrium with atmospheric CO_2, because when brought into contact with water, it dissolves until equilibrium is reached, so that $CO_{2(gas)}$ - $CO_{2(aq)}$. The equilibrium for this reaction lies far to the left.

In soils, CO_2 is set free during respiration and oxidation of organic matter. This causes the CO_2 in soil air to reach values of some volume percent corresponding to a partial pressure, $pCO_2 \approx 10^{-2}$ atm. Thus, subsurface flow outcropping in, for example, small river channels like *La Trucha,* is usually supersaturated in CO_2.

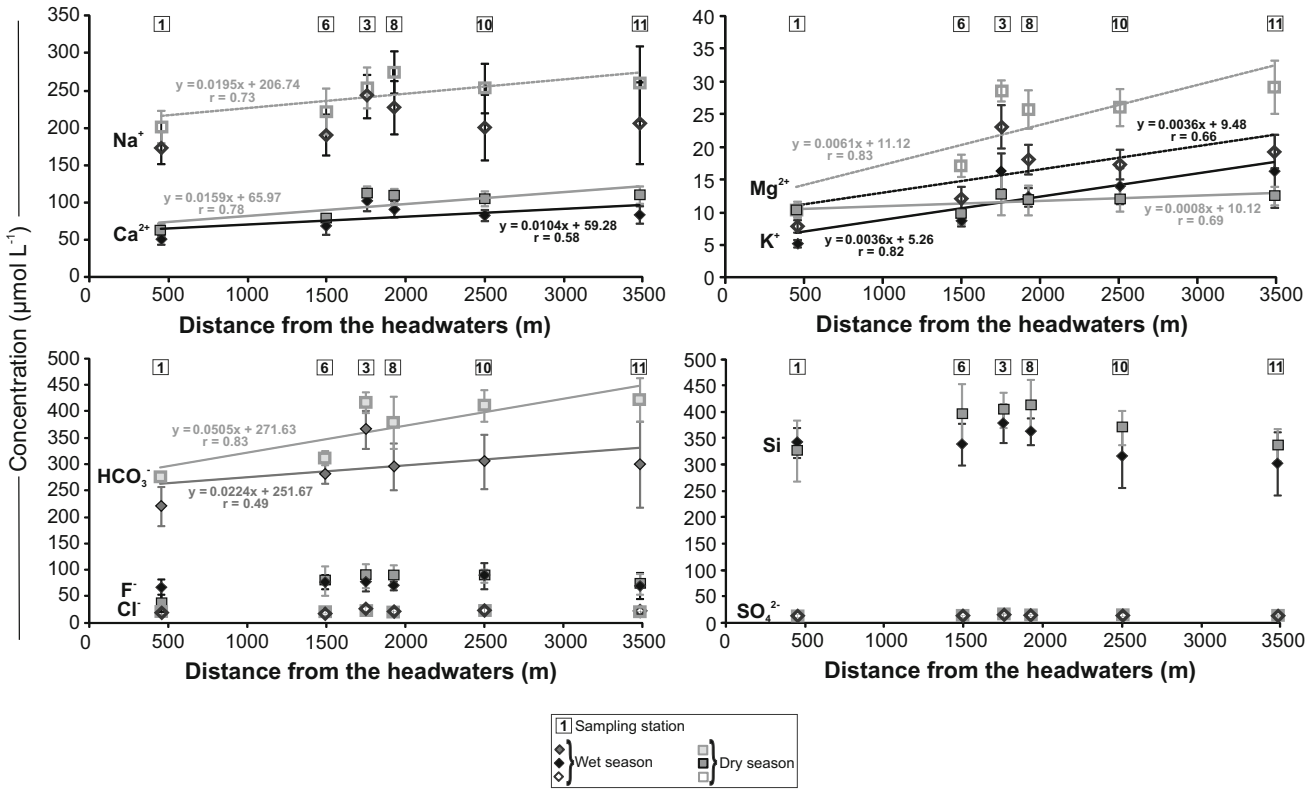

Fig. 10 Downstream seasonal variation of the concentration of major ions and silicon at *La Trucha* catchment

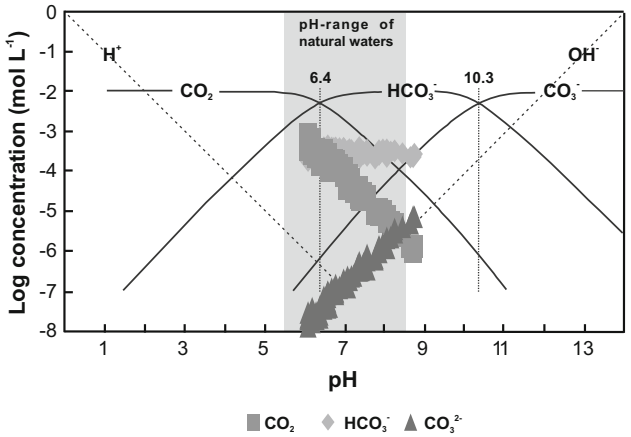

Fig. 11 Bejrrum diagram showing the pH dependency of the speciation of dissolved inorganic carbon species (DIC) at *La Trucha* catchment

Dissolved inorganic carbon (DIC) has been defined as $DIC = CO_{2(aq)} + HCO_3^- + CO_3^{2-}$ (e.g., Stumm and Morgan 1996). Because carbonate alkalinity is frequently close to zero and, also, because only a small fraction of $CO_{2(aq)}$ reacts with water ($CO_{2(aq)} + H_2O \leftrightarrow H_2CO_3$), approximately 80–90 % of DIC is bicarbonate with the balance being $CO_{2(aq)}$. This is clearly shown in the Bjerrum plot (Fig. 11), where the speciation of *La Trucha*'s inorganic carbon system is shown as a function of pH. The molar concentration of each carbon species was calculated with PHREEQC (Parkhurst and Appelo 2013).

Alkalinity, on the other hand, results from silicate hydrolysis, with a lesser contribution from carbonate dissolution and, to a smaller extent, from the synthesis of organic matter. There is a significant correlation (Fig. 12a) between alkalinity and conductivity in the analyzed stream waters ($r = 0.82$; $p < 0.001$), revealing that over 67 % of the variance of electrical conductivity is accounted for alkalinity. The waters from sub-basin A exhibit the lowermost values for both parameters, whereas the highest values were measured in spring waters. Springs flowing into the stream from sub-basin B affect its chemical signature, mainly during (austral) winter. In this sense, they supply significant amounts of dissolved inorganic carbon, as their DIC concentrations are 1.5–1.9 times higher than in surface waters. Conversely, DIC shows a significant negative correlation with pH ($r = -0.75$; $p < 0.001$) in the watershed (Fig. 12b). This suggests that DIC, which accounts for over 56 % of pH's variance, is mainly consumed to synthesize biomass, and water becomes more alkaline (e.g., Manahan 2000), through reactions of the type:

$$106\ CO_2 + 16\ NO_3^- + HPO_4^{2-} + 122\ H_2O + 18\ H^+ \leftrightarrow \{C_{106}H_{263}O_{110}N_{16}P_1\} + 138\ O_2$$

In this reaction, photosynthesis rules if equilibrium moves to the right-hand side of the equation, and

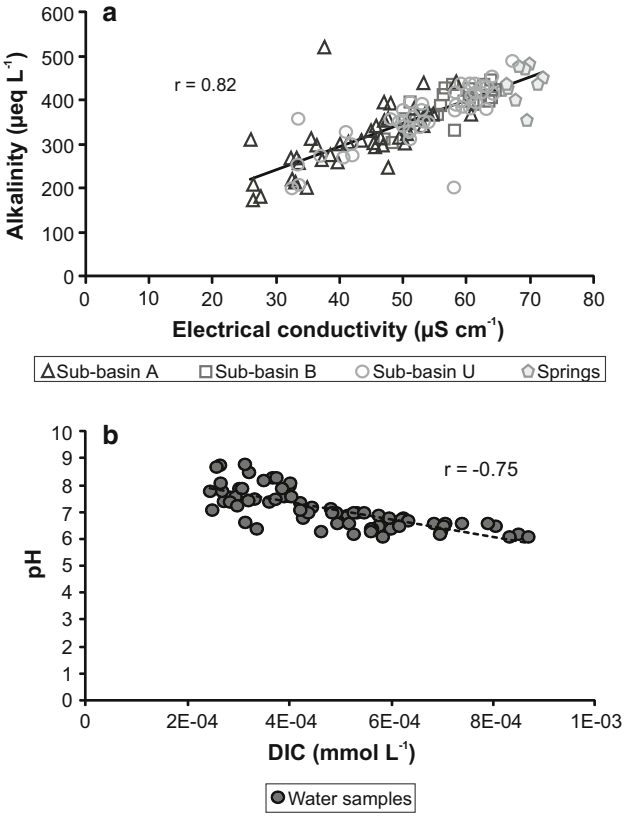

Fig. 12 **a** Alkalinity vs. electrical conductivity in stream waters from *La Trucha*. **b** pH vs. dissolved inorganic carbon (DIC) in the catchment

respiration is preeminent if equilibrium moves to the left (Stumm and Morgan 1996).

Inorganic carbon also exhibits seasonal variations, reaching maximum concentrations in October (0.73 µmol L^{-1}) and minimum concentrations in March (0.33 µmol L^{-1}). The highest HCO_3^- concentrations were recorded during the dry season, whereas $CO_{2(aq)}$ increases during the rainy season, mainly between September and February, reaching ~40 % of carbon species during such period (Fig. 13a). In contrast, between March and August—the dry season—the $CO_{2(aq)}$ contribution to DIC decreases to ~19 % (Fig. 13b). The aqueous CO_2 sources can be allochthonous (i.e., soil $CO_{2(gas)}$, which is produced by mineralization/decomposition of terrestrial organic matter and root respiration of plants) or autochthonous (i.e., CO_2 from in situ respiration of aqueous organic carbon, photodegradation of dissolved organic matter, and carbonate precipitation) (e.g., Li et al. 2012). Remarkably, in the case of the studied watershed, maximum $CO_{2(aq)}$ concentrations are recorded in (austral) summer, associated with an increase in ambient temperature, biological activity, and rainfall. Furthermore, a conspicuous spring water CO_2 degasification was chemically measured in the stream, after discharging into sub-basin B.

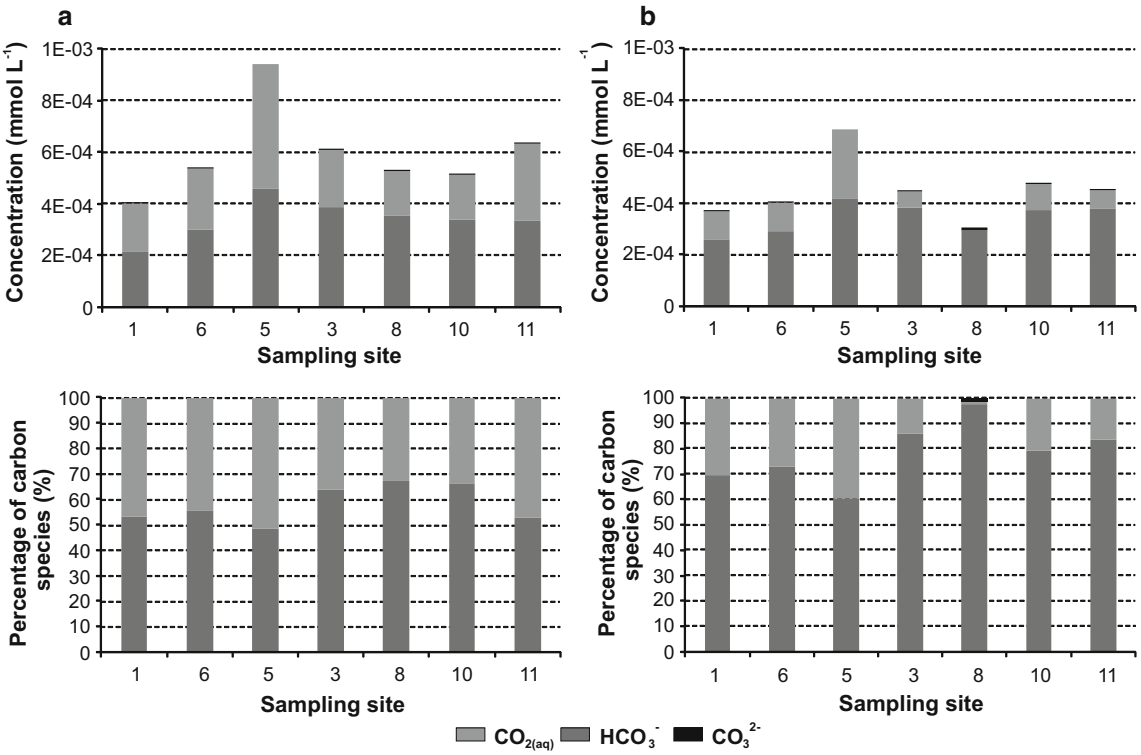

Fig. 13 Dissolved inorganic species distribution in sampling stations from *La Trucha*. **a** Between September and February. **b** Between March and August

Mountainous rivers tend to have very low concentrations of dissolved organic carbon (DOC), typically around 1 mg L^{-1} (Berner and Berner 1987). About half of the DOC in rivers is fulvic acid, which is the fraction of humic substances soluble in the entire pH spectrum found in rivers (e.g., Wohl 2010). During the dry season (austral winter), DOC concentration at *La Trucha* was 1.32 ± 0.25 mg L^{-1}, and it increased during the wet season (i.e., due to rainfall-induced DOC mobilization), reaching 2.92 ± 0.64 mg L^{-1} (Table 1). The labile part (i.e., mainly carbohydrates and amino acids), which usually a small proportion of DOC, is surely oxidized and converted into dissolved $CO_{2(aq)}$. Similar observations have been made in a comparable fluvial system of the *Sierras Pampeanas* of Córdoba (Argentina) (Gaiero et al. 1998).

Almost all rivers have a much higher pCO_2 than the atmosphere because of the in situ respiration of labile organics (e.g., Kempe 1982). In the study area, groundwater input is probably the main source of $CO_{2(aq)}$, because it usually has much higher $CO_{2(aq)}$ concentrations than surface waters due to its link to chemical weathering and the soil zone (e.g., Schulte et al. 2011). Regardless of the origin of this CO_2 overpressure, most rivers degas the CO_2 to the atmosphere (e.g., Butman and Raymond 2011). This CO_2 evasion causes the pCO_2 to decrease downflow, as seen, for example, in large rivers, like the Amazon (Richey et al. 2002) and the Nyong (Brunet et al. 2009). This pattern, however, may not be evident in small mountainous watersheds, such as *La Trucha*, since the major contributors to the main stream are the first-order tributaries, which exhibit high pCO_2.

Butman and Raymond (2011) have shown in their study of CO_2 efflux of streams and rivers in the conterminous USA, that there is a clear dominance of supersaturation with respect to the atmosphere. Furthermore, the partial pressure of CO_2 was found to decrease as a function of stream order and, also, their modeling predicted that gas transfer velocities were highest in streams of the first and second order.

La Trucha is a second-order stream subjected to an intensive *weathering-limited* regime, because the *Sierra de Comechingones* has undergone a significant exhumation since the Late Cretaceous (Campodonico et al. 2014 and references therein). Therefore, most of its surface area is composed of exposed fractured granite and sparse sediment accumulations in topographic lows. This environmental characteristics lead to a priori assessment that the first- and second-order streams in the *Achala* Batholith are not significant CO_2 providers to the atmosphere.

The use of PHREEQC inverse models have shown that in *La Trucha*, CO_2 is the most significant exchanged phase. Gas transfer velocity has proved to be a function of

turbulence at the air–water interface (Butman and Raymond 2011), and this characteristic was evident through chemical analyses and modeling at *La Trucha*, where $CO_{2(aq)}$, in the upper and steeper catchment, was the most abundant species in summer (3.18×10^{-4} mmol kg^{-1} $_{water}$, or 39 % of the participating chemical species) and in winter (5.81×10^{-4} mmol kg^{-1} $_{water}$, or 57 % of the participating species). The significance of the overall *La Trucha* carbon exchange scheme becomes evident when the mean molar exchanges for the entire catchment are considered: CO_2 constitutes 66 % of all exchanged phases during the dry winter season and 39 % during the rainy summer.

These concentrations lead to an estimate of the mean carbon efflux for *La Trucha* catchment in $\sim$180 mg C m^{-2} $year^{-1}$. It has been estimated that the first- and second-order catchments occupy about 2.5 % ($\sim$62.5 km^2) of the *Achala* Batholith's surface area. Butman and Raymond (2011) have shown that the first- and second-order streams reach the highest mean CO_2 partial pressure in their study of the conterminous USA. Future studies in Argentina's *Sierras Pampeanas* should extend the investigation of carbon dynamics to other lithologies and higher order streams.

Concluding comments

The second-order catchment, known as *La Trucha* in the *Sierra de Comechingones* in Central Argentina, was chosen to develop a pilot study that would allow to probe into the mechanisms governing surface geochemistry in the *Achala* Batholith. The first part of the study (Campodonico et al. 2014) clearly showed that the mountainous, fluorine-rich granitic area is controlled by a *weathering-limited regime*, where physical processes are more important than chemical ones in the weathering scenario. Ensuing denudation transports and selects debris into a fairly coarse regolith (enriched in potassium feldspar and quartz) and a finer fraction that accumulates in topographic depressions and supplies most dissolved solids. The dissolved phase is provided by the hydrolysis of plagioclase, biotite, and apatite. Statistical analysis showed that significant losses occur in the fine grain-size regolith and involve MgO, MnO, and P_2O_5. The *chemical index of weathering* (CIW) (Harnois 1988) reflected incipient weathering: a mean and standard deviation of 69.6 ± 3.7 for the country rock against 70.7 ± 0.5 for the fine-grained regolith.

The main dissolved chemical characteristics of *La Trucha* are coherent with the F-rich granitic terrain: the chemical composition was dominated by Na^+, Ca^{2+}, HCO_3^-, and F^-, which accounted for $\sim$89 and $\sim$90 % of the total concentration of major cations and anions, respectively. The relatively high dissolved concentrations of F^- are explained by the hydrolysis of fluorapatite and biotite. Furthermore, the analysis of the resulting dissolved chemical data shows that these minerals are led by oligoclase, as a major solute provider. The dissolution of calcite (partly allochthonous?) is another likely source of Ca^{2+} and alkalinity. It must be emphasized here that, the two first-order streams (i.e., A and B) that supply water to *La Trucha*'s main stem differ in terms of slope, area, length, and volume of accumulated sediment. These characteristics are translated into a different chemical response: A, which is larger, longer, less steep than B, and appears to have a smaller sediment volume, and delivers a lower alkalinity and TDS load.

Although in terms of climate, there are four clearly distinguishable seasons in the *Sierra de Comechingones*, there are only two from the atmospheric precipitations point of view: rainy (October until March) and dry (April until September). Most major chemical components are subjected to dilution during the wet season due to high discharges. Thus, Na^+, Ca^{2+}, Mg^{2+}, HCO_3^-, SO_4^{2-}, and F^- are less concentrated during summer. Chloride is a conservative element and is clearly controlled by the chemical composition of rainfall. The rainfall-induced mobilization of K^+ is likely masked by its affinity for adsorption onto fine-grained particles. Likewise, SiO_2 is consumed by algae and freshwater sponges.

The contribution of subsurface flow determines the stream increase in its electrical conductivity less rapidly (3.9 μS cm^{-1} per 1000 m) in rainy summer than in dry winter (6.7 μS cm^{-1} per 1000 m), when subsurface flow is more concentrated. The electrical conductivity of rainfall, on the other hand, is significant, with a mean of 19.1 μS cm^{-1} for the January–February 2006 rainy period. It follows that the residence time of subsurface flow within rock fractures and in the accumulated regolith is long enough to almost double the concentrations of solutes.

Alkalinity and conductivity are significantly correlated ($r = 0.82$; $p < 0.001$), revealing that over 67 % of the variability of conductivity is accounted for alkalinity. DIC shows seasonal variations, reaching maximum concentrations in October (0.73 μmol L^{-1}) and minimum concentrations in March (0.33 μmol L^{-1}). With some variability, CO_2 is mobilized by rainfall, because $CO_{2(aq)}$ increases its concentration in the stream between September and February, reaching $\sim$40 % of carbon species during such period. In contrast, during the dry season, only $\sim$19 % of DIC is composed of $CO_{2(aq)}$. It should be emphasized that although DOC concentrations in *La Trucha* are low (1.32 ± 0.25 mg L^{-1} during the dry season, and 2.92 ± 0.64 mg L^{-1} during the wet season), the labile fraction of such DOC is surely partially oxidized and converted into $CO_{2(aq)}$.

The inverse models (i.e., using PHREEQC) allowed the calculation of free CO_2 and, therefore, the likelihood of its

evasion in different seasons and areas of the catchment. A mean carbon efflux of $\sim$180 mg C m^{-2} $year^{-1}$ has been estimated for *La Trucha* catchment. As the first- and second-order streams, which occupy about 2.5 % ($\sim$62.5 km^2) of the *Achala* Batholith's surface area, are the most significant stretches in the carbon exchange scheme, more work must be added to have a more accomplished image of the whole process in this batholith.

Acknowledgments The authors wish to acknowledge the continued support of the Universidad Nacional de Córdoba (UNC) and Argentina's Consejo Nacional de Investigaciones Científicas y Técnicas (CONICET). Thanks are also extended to the personnel of *La Domanda* inn for the valuable assistance provided during the development of the field work. The comments of two anonymous reviewers have helped to improve the original version of this MS.

References

April R, Newton R, Coles LT (1986) Chemical weathering in two Adirondack watershed: past and present-day rates. Geol Soc Am Bull 97:1232–1238

Berner EK, Berner RA (1987) The global water cycle: geochemistry and environment. Prentice Hall, Englewood Cliffs

Berner RA, Lasaga AC, Garrels RM (1983) The carbon-silicate geochemical cycle and its effect on atmospheric carbon dioxide over the past 100 million years. Am J Sci 283:641–683

Brunet F, Dubois K, Veizer J, Ndondo GRN, Ngoupayou JRN, Boeglin JL, Probst J-L (2009) Terrestrial and fluvial carbon fluxes in a tropical watershed: Nyongbasin, Cameroon. Chem Geol 265:563–572

Butman D, Raymond PA (2011) Significant efflux of carbon dioxide from streams and rivers in the United States. Nat Geos. doi:10.1038/NGEO1294

Campodonico VA, Martínez JO, Verdecchia SO, Pasquini AI, Depetris PJ (2014) Weathering assessment in the Achala Batholith of the Sierra de Comechingones, Córdoba, central Argentina. I: granite-regolith fractionation. Catena 123:121–134

Capitanelli RG (1979) Geomorfología. In: Vázquez JB et al (eds) Geografía física de la Provincia de Córdoba. Boldt, Córdoba

Carignano CA, Cioccale MA, Rabassa J (1999) Landscape antiquity of the central-eastern Sierras Pampeanas (Argentina): geomorphological evolution since Gonwandic times. Z Geomorphol Ann Geomorph 118:245–268

Carson MA, Kirkby NJ (1972) Hillslope form and processes. Cambridge University Press, Cambridge

Daga C, Soteras F, Daniele GM, Domínguez LS (2014) New records of freshwater algae and cyanobacteria from mountain streams of Córdoba (Argentina). Bol Soc Argent Bot 49(4):447–456

Depetris PJ, Pasquini AI, Lecomte KL (2014) Weathering and the riverine denudation of continents, Springer Briefs in Earth System Science. Springer, Berlin

Drever JI (1988) The geochemistry of natural waters, 2nd edn. Prentice-Hall, New Jersey

Eaton AD, Clesceri LS, Greenberg AE (1995) Standard methods for the examination of water and wastewater. A.P.H.A./A.W.W.A./W.E.F, Washington DC

Gaiero DM, Depetris PJ, Kempe S (1998) Carbon dynamics in a medium-size semiarid basin: the Suquía River, Córdoba (Argentina). Min Mag 62A:487–488

Gaillardet J, Dupré B, Louvat P, Allegre CJ (1999) Global silicate weathering and CO_2 consumption rates derived from the chemistry of large rivers. Chem Geol 159:3–30

Gari N, Corigliano M (2004) La estructura del perifiton y de la deriva algal en arroyos serranos. Limnetica 23(1–2):11–24

Harnois L (1988) The CIW index: a new chemical index of weathering. Sediment Geol 55:319–322

Horton RE (1945) Erosional development of streams and their drainage basins. Hydrophysical approach to quantitative morphology. Geol Soc Am Bull 56:275–370

Isacks BL (1988) Uplift of the Central Andean Plateau and bending of the Bolivian orocline. J Geophys Res 93(B4):3211–3231

Kempe S (1982) Long-term records of CO_2 pressure fluctuations in fresh water. In: Degens ET (ed) Transport of carbon and minerals in major world rivers. Mitteilungenaus dem Geologisch-Paläontologischen Institut der Universität Hamburg, vol 52, Hamburg, pp 91–332

Lecomte KL, Pasquini AI, Depetris PJ (2005) Mineral weathering in a semiarid mountain river: its assessment through PHREEQC inverse modeling. Aquat Geochem 11:173–194

Lecomte KL, García MG, Fórmica SM, Depetris PJ (2009) Influence of geomorphological variables on mountainous stream water chemistry (Sierras Pampeanas, Córdoba, Argentina). Geomorphology 110:195–202

Lecomte KL, García MG, Fórmica SM, Depetris PJ (2011) Hidroquímica de ríos de montaña (Sierras de Córdoba, Argentina): elementos mayoritarios disueltos. Lat Am J Sedimentol Basin Anal 18(1):43–62

Li S, Lu XX, He M, Zhou Y, Li L, Ziegleret AD (2012) Daily CO_2 partial pressure and CO_2 outgassing in the upper Yangtze River basin: a case study of the Longchuan River, China. J Hydrol 466–467:141–150

Lira R, Kirschbaum AM (1990) Geochemical evolution of granites from the Achala Batholith of the Sierras Pampeanas, Argentina. Geol Soc Am Spec Papers 241:67–76

Manahan SE (2000) Environmental Chemistry, 7th edn. Lewis Publisher/CRC Press, Boca Raton

Manning JC (1987) Applied principles of hydrology. Merrill, Columbus

Meybeck M (2005) Global occurrence of major elements in rivers. In: Drever JI (ed) Surface and ground water, weathering, and soils. Elsevier, Amsterdam, pp 207–223

Oliva P, Viers J, Dupré B (2003) Chemical weathering in granitic environments. Chem Geol 202:225–256

Oliva P, Dupré B, Martin F, Viers J (2004) The role of trace minerals in chemical weathering in a high-elevation granitic watershed (Estibère, France): chemical and mineralogical evidence. Geochim Cosmochim Acta 68:2223–2244

Parkhurst DL, Appelo CA (2013) Description of input and examples for PHREEQC version 3—a computer program for speciation, batch-reaction, one-dimensional transport, and inverse geochemical calculations. U.S. Geological Survey Techniques and Methods, book 6, chap. A43

Pasquini AI, Lecomte KL, Piovano EL, Depetris PJ (2006) Recent rainfall and runoff variability in central Argentina. Quat Int 158:127–139

Piper AM (1944) A graphic procedure in the geochemical interpretation of water analyses. Am Geophys Union Trans 25:914–923

Rapela CW, Baldo EG, Pankhurst RJ, Fanning CM (2008) The Devonian Achala Batholith of the Sierras Pampeanas: F-rich, aluminous A-type granites. In: Proceedings of VI South American symposium on isotope geology, pp 1–8

Richey JE, Melack JM, Aufdenkampe AK, Ballester VM, Hess LL (2002) Outgassing from Amazonian rivers and wetlands as a large tropical source of atmospheric CO_2. Nature 416:617–620

Schulte P, van Geldern R, Freitag H, AjazKarim A, Négrel P, Petelet-Giraud E, Probst A, Probst J-L, Telmer K, Veizer J, Barth JAC (2011) Applications of stable water and carbon isotopes in watershed research: weathering, carbon cycling, and water balances. Earth Sci Rev 10:20–31

Serrano SE (1997) Hydrology for engineers, geologists and environmental professionals. Hydro Science Inc., Lexington

Siegesmund S, Steenken A, Martino RD, Wemmer K, López de Luchi MG, Frei R, Presnyakov S, Guereschi AB (2010) Time constrains on the tectonic evolution of the Eastern Sierras Pampeanas (central Argentina). Int J Earth Sci 99:1199–1226

Strahler AN (1952) Hypsometric (area altitude) analysis of erosional topology. Geol Soc Am Bull 63:117–1142

Stumm W, Morgan JJ (1996) Aquatic chemistry. Chemical equilibrium and rates in natural waters, 3rd edn. Wiley-Interscience, New York

White AF, Bullen TD, Vivit DV, Schulz M, Clow DW (1999) The role of disseminated calcite in the chemical weathering of granitoid rocks. Geochim Cosmochim Acta 63:1939–1953

Wohl E (2010) Mountain rivers revisited. American Geophysical Union, Washington DC